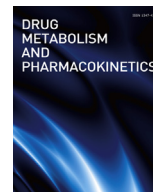




Contents lists available at ScienceDirect

## Drug Metabolism and Pharmacokinetics

journal homepage: <http://www.journals.elsevier.com/drug-metabolism-and-pharmacokinetics>

## Regular Article

## Synthesis and evaluation of nevirapine analogs to study the metabolic activation of nevirapine

Yasuhiro Tateishi <sup>a</sup>, Tomoyuki Ohe <sup>a,\*</sup>, Daisuke Yasuda <sup>a</sup>, Kyoko Takahashi <sup>a</sup>, Shigeo Nakamura <sup>b</sup>, Yasuhiro Kazuki <sup>c,d</sup>, Tadahiko Mashino <sup>a,\*\*</sup><sup>a</sup> Faculty of Pharmacy, Keio University, 1-5-30 Shibakoen, Minato-ku, Tokyo, Japan<sup>b</sup> Department of Chemistry, Nippon Medical School, 1-7-1 Kyonan-cho, Musashino, Tokyo, Japan<sup>c</sup> Department of Biomedical Science, Institute of Regenerative Medicine and Biofunction, Graduate School of Medical Science, Tottori University, 86 Nishi-cho, Yonago, Tottori, Japan<sup>d</sup> Chromosome Engineering Research Center (CERC), Tottori University, 86 Nishi-cho, Yonago, Tottori, Japan

## ARTICLE INFO

## Article history:

Received 19 September 2019

Received in revised form

19 December 2019

Accepted 29 January 2020

Available online 28 February 2020

## Keywords:

Nevirapine

Metabolic activation

Cytochrome P450

Hepatotoxicity

HepG2

## ABSTRACT

Nevirapine (NVP) is widely used as a non-nucleoside reverse transcriptase inhibitor of HIV-1, however, it is associated with severe skin and liver injury. The mechanisms of these adverse reactions are not yet clear, but the metabolic activation of NVP is thought to be related to the injury process. Until now, several metabolic activation pathways of NVP have been reported. In this study, in order to identify the reactive metabolite of NVP mainly responsible for CYP inhibition and liver injury, we synthesized five NVP analogs designed to avoid the proposed bioactivation pathway and evaluated their metabolic stabilities, CYP3A4 time-dependent inhibitory activities, and cytotoxicity. As a result, only a pyrimidine analog of NVP, which could avoid the formation of a reactive epoxide intermediate, did not inhibit CYP3A4. Outside of this compound, the other synthesized compounds, which could avoid the generation of a reactive quinone-methide intermediate, inhibited CYP3A4 equal to or stronger than NVP. The pyrimidine analog of NVP did not induce cytotoxicity in HepG2 and transchromosomal HepG2 cells, expressing major four CYP enzymes and CYP oxidoreductase. These results indicated that the epoxide intermediate of NVP might play an important role in NVP-induced liver injury.

© 2020 The Japanese Society for the Study of Xenobiotics. Published by Elsevier Ltd. All rights reserved.

## 1. Introduction

Nevirapine (NVP, Fig. 1) is the first nonnucleoside reverse transcriptase inhibitor widely used for the combination treatment of HIV-1 infections, particularly in developing countries because of its ease of use and low cost. Despite its effectiveness, NVP is associated with severe liver and skin injuries, which occur with an incidence of 1.0 and 0.3%, respectively [1]. Although it was reported that NVP itself inhibits human hepatocyte growth [2] or induces apoptosis and mitochondrial dysregulation in HepG2 cells [3,4],

these adverse drug reactions are thought to be associated with the metabolic activation of NVP described below.

In humans, NVP is metabolized by cytochrome P450 (CYP) and is mainly excreted in the urine. An *in vivo* study showed that the metabolites of NVP that are detected in human urine are the glucuronide conjugates of 2-, 3-, 8-, and 12-hydroxyNVP [5]. It was also reported that CYP3A4 and CYP2B6 are responsible for the formation of Phase I NVP metabolites; the former is involved in the formation of 2- and 12-hydroxyNVP and the latter catalyzes 3- and 8-hydroxyNVP [6]. 12-HydroxyNVP (12-OH-NVP) is further metabolized by sulfotransferase 1A1 (SULT1A1) to yield 12-sulfoxyNVP [7] or is oxidized to form 4-carboxyNVP [8].

Evidence for the *in vivo* bioactivation of NVP was also reported where NVP could adduct with human serum albumin or hemoglobin [8,9], or two NVP mercapturates substituted at the C-3 and C-12 positions were identified, suggesting the possibility of the metabolic activation of NVP in humans [10]. Although various bioactivation pathways of NVP have been investigated to date, it is generally recognized that 12-OH-NVP is a key metabolite related to

**Abbreviations:** NVP, nevirapine; CYP, cytochrome P450; 12-OH-NVP, 12-hydroxyNVP; SULT1A1, sulfotransferase 1A1; TC-HepG2, transchromosomal HepG2; G6P, glucose-6-phosphate; G6PDH, G6P dehydrogenase; HLM, human liver microsomes; LC-MS, liquid chromatography with mass spectrometry; BSO, L-butathionine-S,R-sulfoximine; AFT, aflatoxin B1; SIM, selected ion monitoring.

\* Corresponding author.

\*\* Corresponding author.

E-mail address: [ohetm@pha.keio.ac.jp](mailto:ohetm@pha.keio.ac.jp) (T. Ohe).<https://doi.org/10.1016/j.dmpk.2020.01.006>

1347-4367/© 2020 The Japanese Society for the Study of Xenobiotics. Published by Elsevier Ltd. All rights reserved.

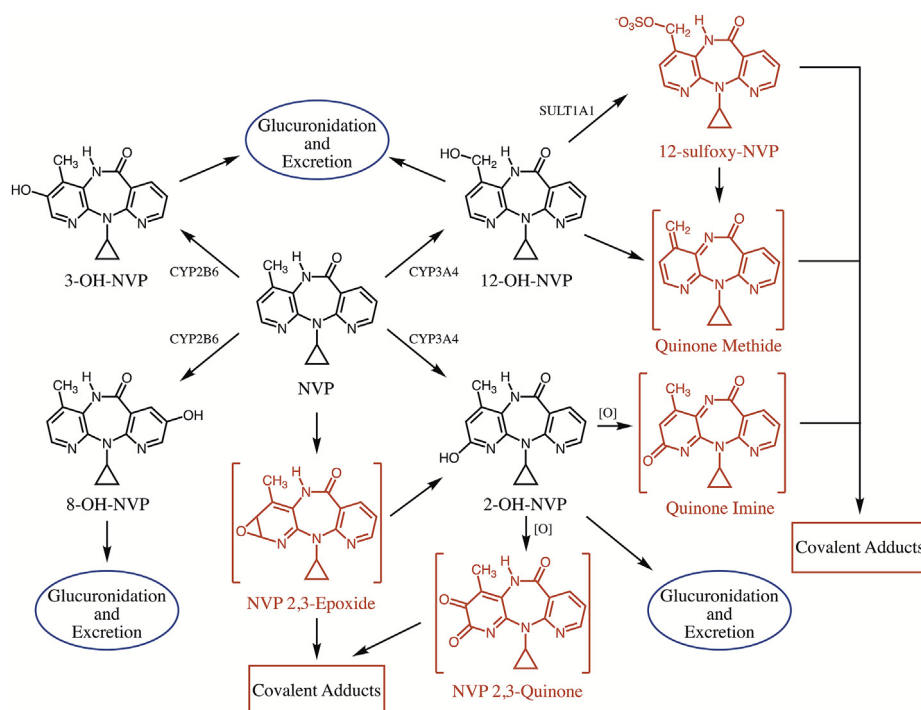


Fig. 1. Structure of NVP and its proposed bioactivation pathways.

NVP-induced toxicity. Chen et al. proposed that the reactive quinone-methide formed from 12-OH-NVP is responsible for skin rashes [7]. Other studies showed that 12-sulfoxyNVP formed from 12-OH-NVP is also related to NVP-induced skin rashes [11,12]. Furthermore, 12-OH-NVP causes upregulation of various genes in the skin that induce immune reactions leading to skin rashes [13]. Recently, Fang et al. demonstrated that 12-sulfoxyNVP formed adducts with deoxynucleosides and amino acids [14].

Bioactivation of NVP also appears to be the cause of liver injuries. Unlike the skin injury, several reactive metabolites were reported for the liver injury. It was suggested that the quinone-methide metabolite might contribute to NVP-induced liver injuries [15]. On the other hand, not only quinone-methide or 12-sulfoxyNVP produced from 12-OH-NVP but other reactive metabolites such as quinone-imine, 2,3-NVP-quinone, and NVP-2,3-epoxide have also been reported (Fig. 1) [7,15,16]. These metabolites may covalently bind to proteins and ultimately cause liver injuries.

In this study, for the purpose of determining the metabolic activation pathway involved during hepatotoxicity, we synthesized five NVP analogs (1–5, Fig. 2) designed to restrict the formation of quinone-methide, quinone-imine, quinone and epoxide intermediates in the NVP A-ring (methylpyridine ring) which is known to be metabolically activated as described above. Following this, we evaluated the CYP3A4 time-dependent inhibitory activity

of NVP and its analogs as an index of metabolic activation. In addition, the hepatotoxicity of all the produced compounds was assessed using transchromosomal HepG2 (TC-HepG2) cells expressing major CYP enzymes (CYP2C9, CYP2C19, CYP2D6, and CYP3A4) and CYP oxidoreductase [17]. Our data suggests that NVP-2,3-epoxide, together with the reactive quinone-methide metabolites, may play an important role in NVP-induced liver toxicity.

## 2. Materials and methods

### 2.1. Materials

NADP<sup>+</sup>, glucose-6-phosphate (G6P) and G6P dehydrogenase (G6PDH) were purchased from Roche Diagnostics (Basel, Switzerland). NVP was obtained from Tokyo Chemical Industry (Tokyo, Japan). All other reagents used for microsomal and cytotoxicity experiments were of analytical grade.

### 2.2. Synthesis of NVP analogs

We chemically synthesized NVP derivatives **1**, **2** and novel NVP analogs **3–5** as shown in Fig. 3. Briefly, for the synthesis of **1** or **5**, condensation of 3-amino-2-chloropyridine or 4-amino-3-chloro-5-methylpyridazine prepared by methylation and the following amination of 4,5-dichloropyridazine-3(2H)-one, with 2-chloronicotinoyl

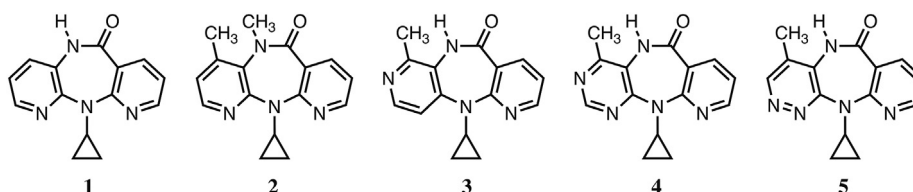
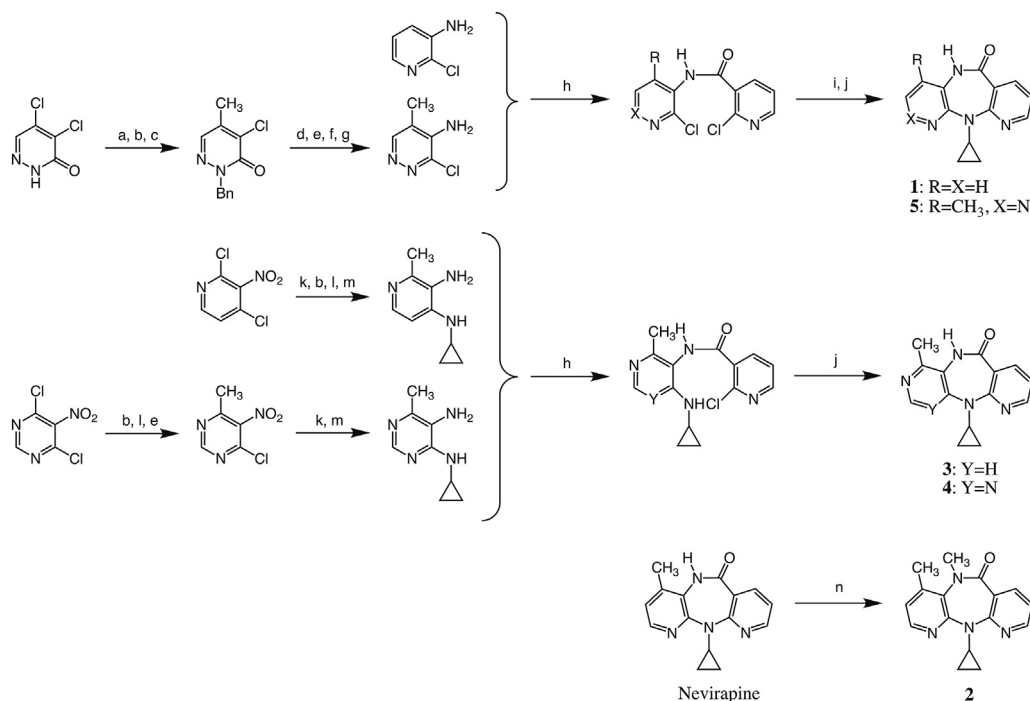


Fig. 2. Chemical structures of the synthesized NVP analogs.



**Fig. 3. Synthesis of NVP analogs.** Reagents and Conditions; (a) BnBr, K<sub>2</sub>CO<sub>3</sub>, DMF, rt, 20 h; (b) dimethyl malonate, <sup>t</sup>BuOK, THF, rt (0.3 h)-reflux (1.5–3.5 h); (c) conc. HCl, reflux, 2 h, then KF, H<sub>2</sub>O, DMF, 170 °C, 3 h; (d) AlCl<sub>3</sub>, toluene, 50 °C, 20 min; (e) POCl<sub>3</sub>, reflux, 1–2 h; (f) NaN<sub>3</sub>, DMF, 50 °C, 2.5 h; (g) NaBH<sub>4</sub>, THF/CH<sub>3</sub>OH, rt, 0.5 h; (h) 2-chloronicotinoyl chloride, NaH or pyridine, THF or DMF, 0 °C–rt, 1–3 h; (i) cyclopropylamine, K<sub>2</sub>CO<sub>3</sub>, toluene/DMF or DMSO, 120 °C, 4.5–22 h; (j) NaH, toluene/DMF, reflux, 2–23 h; (k) cyclopropylamine, triethylamine or K<sub>2</sub>CO<sub>3</sub>, THF or toluene, rt–120 °C, 0.2–15.5 h; (l) conc. HCl, reflux, 1–1.5 h; (m) H<sub>2</sub>, Pd/C, CH<sub>3</sub>OH, rt, 12–19.5 h; (n) NaH, DMF, 60 °C, 2 h, then CH<sub>3</sub>I, DMF, rt, 2 h.

chloride gave nicotinamides. These amides were reacted with cyclopropylamine, followed by ring closure to produce **1** or **5**. In the case of compounds **3** and **4**, condensation of diaminopyridine or diaminopyrimidine prepared stepwise from 2,4-dichloro-3-nitropyridine or 4,6-dichloro-5-nitropyrimidine as a starting material, with 2-chloronicotinoyl chloride gave nicotinamides, and the following ring closure reaction produced compounds **3** or **4**. Compound **2** was synthesized by direct *N*-methylation of NVP using methyl iodide. More detailed procedures and analytical data for the synthesized compounds are shown in the [Supplemental Data](#).

### 2.3. Metabolic stability in liver microsomes

Pooled human (200 donors) liver microsomes (HLM) were purchased from XenoTech (Lenexa, KS). All incubations were conducted at 37 °C in a water bath. Stock solutions of the test compounds were prepared in methanol. The incubation mixtures containing HLM (0.4 mg protein/mL), the test compounds (1 μM), MgCl<sub>2</sub> (3 mM), G6P (10 mM), and G6PDH (2 unit/mL) in 0.5 mL of 0.1 M K-Pi buffer (pH 7.4) were preincubated for 3 min. The reaction was initiated by adding NADP<sup>+</sup> (1 mM) and then incubated for 30 min. The reaction was stopped by the addition of 1 mL of an ice-cold mixed acetonitrile/methanol (2/1) solution containing 1 μM cortisone. The mixture was centrifuged at 10,000×g for 10 min. The supernatant (20 μL) was injected and analyzed by liquid chromatography with mass spectrometry (LC-MS, 6120; Agilent Technologies, Palo Alto, CA). The HPLC mobile phase A was water with 0.1% formic acid, and mobile phase B was acetonitrile with 0.1% formic acid. Chromatographic separations were performed using an InertSustain C18 column (4.6 × 100 mm, 3.0 μm; GL Sciences, Tokyo, Japan) at a flow rate of 0.5 mL/min under the following

gradient elution profile: 30% solvent B for 1 min, 30–100% B in 5 min, 100% B for 4 min, then 100 to 30% B in 0.1 min followed by 30% B for another 3.9 min (15 min in total). The eluent was introduced directly into the mass spectrometer via electrospray ionization using the positive ion mode.

### 2.4. CYP inactivation

According to reported procedures [18], midazolam 1'-hydroxylase activity was determined to quantify the time-dependent loss of CYP3A4 activity of HLM in the presence of NVP and its analogs. In brief, primary incubations included 100 μM of the following test compounds, 1 mM NADP<sup>+</sup>, 10 mM G6P, 2 unit/mL G6PDH, 1 mg/mL HLM, 3 mM MgCl<sub>2</sub>, and 0.1 M K-Pi buffer (pH 7.4). The mixtures were incubated for 30 min. Then, 50 μL aliquots of the primary incubation mixtures were transferred to a secondary incubation with a final volume of 0.5 mL, which included 40 μM midazolam, 1 mM NADP<sup>+</sup>, 10 mM G6P, 2 unit/mL G6PDH, 3 mM MgCl<sub>2</sub>, and 0.1 M K-Pi buffer (pH 7.4). The midazolam mixture was incubated for 10 min and stopped by the addition of 1 mL of an ice-cold mixed acetonitrile/methanol (2/1) solution containing 1 μM cortisone. The mixture was then centrifuged at 10,000×g for 10 min. The supernatant (10 μL) was injected and 1'-hydroxymidazolam was quantified by the LC-MS analysis. The CYP3A4 remaining activities (%) of test compounds were calculated as the percentage of the initial activity obtained without preincubation. The CYP3A4 remaining activity of control (treated with solvent only) was also calculated. Then, time-dependent inhibition (%) of CYP3A4 was expressed as the difference between the remaining activities of control and each compound. The equations used for the calculation were shown as follows:

**Table 1**  
Metabolic stability and CYP3A4 time-dependent inhibitory activity of NVP and its analogs.

Compound	Metabolic Stability (% remaining)	CYP3A4 Time Dependent Inhibition (%)
NVP	93.6 ± 7.5	13.8* ± 4.9
<b>1</b>	86.2 ± 4.2	3.9 ± 8.8
<b>2</b>	94.5 ± 3.5	13.3* ± 9.3
<b>3</b>	96.1 ± 4.8	32.6*, † ± 1.8
<b>4</b>	72.2 ± 1.2	0.4† ± 3.7
<b>5</b>	23.6 ± 0.9	43.0*, † ± 4.6

For testing metabolic stability, the test compounds were incubated with HLM for 30 min. The remaining amount of test compounds was expressed as percentages relative to the incubation (–) sample. For the CYP time-dependent assay, CYP3A4 remaining activity (%) in HLM was calculated as the percentage of the initial activity obtained without preincubation. The data show differences between the remaining activities of control (treated with solvent only) and each compound. Each value represents the mean of three samples ± S.D. \*p < 0.01; significantly different from negative control, †p < 0.01; significantly different from NVP, Student's *t*-test.

CYP3A4 remaining activity (%) = (activity with preincubation/activity without preincubation) × 100

Time-dependent CYP3A4 inhibition (%) = CYP3A4 remaining activity of control – CYP3A4 remaining activity of compounds

### 2.5. Cell cultures

Human hepatocarcinoma HepG2 cells were purchased from the American Type Culture Collection (Manassas, VA). TC-HepG2 cells expressing major CYP enzymes involved in drug metabolism (CYP2C9, CYP2C19, CYP2D6, and CYP3A4) and CYP oxidoreductase were previously established [17]. The cells were maintained in Dulbecco's modified Eagle's medium (NAKALAI TESQUE, Inc., Kyoto, Japan) containing 10% fetal bovine serum (GIBCO/Life Technologies, Grand Island, NY) and 1% penicillin-streptomycin (Sigma-Aldrich, St. Louis, MO) in a 5% CO<sub>2</sub> incubator under a humidified atmosphere at 37 °C.

### 2.6. Cytotoxicity assay

Cytotoxicity was assessed by a WST-8 assay using a Cell Counting Kit-8 (CCK-8, Dojindo Laboratories, Kumamoto, Japan). The cells were seeded (1 × 10<sup>4</sup> cells/well) on a 96-well plate (Iwaki/Asahi Techno Glass Corporation, Tokyo, Japan). At the time of seeding, L-buthionine-S,R-sulfoximine (BSO, Sigma) solutions in PBS (200 μM) were added. For the BSO (–) group, the cells were treated with PBS. After 24 h of incubation, the test compounds or aflatoxin B1 (AFT) as the positive control, dissolved in DMSO were added. DMSO only was added for negative control (final DMSO concentration was 0.5% v/v). The cells were incubated with the test compounds for 48 h, and then the CCK-8 solution was added. After another 4 h of incubation, the absorbance at 450 nm was measured (Reference 600 nm) using Infinite M1000 PRO Microplate Readers (TECAN, Männedorf, Switzerland), and the cell viability was determined.

## 3. Results

### 3.1. Metabolic stability of NVP and its analogs

NVP and analogs **1** through **5** were incubated with pooled human liver microsomes. All compounds were detected using selected ion monitoring (SIM) mode, and the metabolic stability was defined as the percentage of parent compounds remaining during the incubation. As shown in Table 1, **1**, **2** and **3** were metabolically stable, while the stability of both the pyrimidine-analog **4** and the pyridazine-analog **5** were lower than NVP.

### 3.2. Time-dependent CYP3A4 inhibition of NVP and its analogs

Time-dependent inhibition of CYP3A4 was calculated as the loss of midazolam 1'-hydroxylase activity compared with the control which was preincubated with only solvent. NVP inhibited CYP3A4 significantly, and the *N*-methyl derivative **2** also showed the same level of inhibitory activity as NVP. Although both the pyridine-analogue **3** and the pyridazine-analog **5** inhibited CYP3A4 more strongly, the pyrimidine-analog **4** showed weaker inhibitory activity when compared with NVP. The desmethyl derivative **1** showed lower inhibitory activity than NVP, but the difference was not statistically significant.

### 3.3. Cytotoxicity of NVP and its analogs in HepG2/TC-HepG2 cells

To evaluate the metabolic activation of NVP and its analogs, the cell toxicity of HepG2/TC-HepG2 cells was assessed by a WST-8 assay. We also evaluated the effects of pretreatment with buthionine sulfoximine (BSO), an inhibitor of glutathione (GSH) biosynthesis, since GSH traps reactive metabolites and detoxifies them. As shown in Fig. 4A, no remarkable differences in cell viabilities between HepG2 and TC-HepG2 cells after the addition of NVP was observed without pretreatment using BSO, while the cell viabilities were significantly lower in TC-HepG2 cells treated with AFT than in the parental HepG2 cells under the same condition. On the other hand, under GSH-depleted conditions with the pretreatment of BSO, the cytotoxicity of NVP in TC-HepG2 cells was significantly stronger than in the HepG2 cells. Based on these results, the cytotoxicity of the synthesized compounds was investigated using GSH-depleted TC-HepG2 cells, as the metabolic activation of compounds can be more sensitively evaluated under these conditions. For a comparison purpose, we also examined the toxicity without the pretreatment of BSO. As shown in Fig. 4B, compounds **3** and **4** were less toxic when compared with NVP, while compounds **2** and **5** had significantly stronger toxicity in the BSO (+) condition. Under the BSO (–) condition, there are no remarkable differences in cell viability among compounds.

## 4. Discussion

As shown in Fig. 1, several bioactivation pathways of NVP were proposed to explain the mechanism of NVP-induced liver and/or skin injury. The purpose of the present study is to identify the reactive metabolite of NVP that is mainly responsible for the time-dependent inhibition of CYP and eventual hepatic toxicity by using chemically synthesized NVP analogs. Several reports suggested that the reactive quinone-methide intermediate might contribute to the toxicity, therefore we first synthesized desmethyl derivative **1** and *N*-methyl derivative **2**, which were previously reported by Hargrave

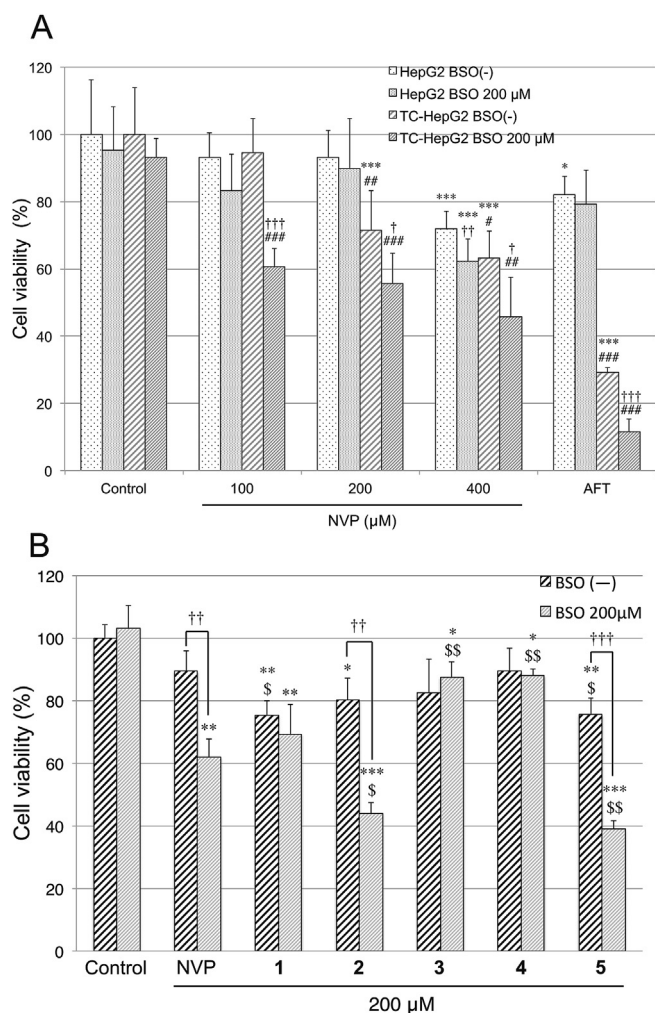


**Fig. 4.** Cytotoxicity to HepG2/TC-HepG2 cells of NVP and its analogs. A: Cytotoxicity in HepG2 or TC-HepG2 cells after 48 h incubation with NVP with or without the pretreatment with BSO (200 μM). Cells were pretreated with PBS (-) for BSO (-) group. The control group was incubated with DMSO. AFT was used as a positive control at 3.3 μM. The bars indicate relative cell viability compared with control of BSO (-) in each cell line. Each value represents the mean of six samples ± S.D. \**p* < 0.05, \*\*\**p* < 0.001; significantly different from each control, †*p* < 0.05, ††*p* < 0.01, †††*p* < 0.001; significantly different from corresponding viability of BSO (-), #*p* < 0.05, ##*p* < 0.01, ###*p* < 0.001; significantly different from corresponding viability of HepG2 cells, Student's *t*-test. B: Cytotoxicity in TC-HepG2 cells after 48 h incubation with NVP and its analogs (200 μM) with or without the pretreatment with BSO (200 μM). Cells were pretreated with PBS (-) for BSO (-) group. The control group was incubated with DMSO. Bars indicate relative cell viability compared with control of BSO (-). Each value represents the mean of three samples ± S.D. \**p* < 0.05, \*\**p* < 0.01, \*\*\**p* < 0.001; significantly different from each control, \$*p* < 0.05, \$\$*p* < 0.01; significantly different from NVP, ††*p* < 0.01, †††*p* < 0.001; significantly different from corresponding viability of BSO (-), Student's *t*-test.

et al. [19] which could avoid the formation of quinone-methide metabolites.

Table 1 shows the metabolic stabilities of **1** and **2** and their CYP3A4 time-dependent inhibitory activities. Although both compounds **1** and **2** were metabolically stable to the same degree as NVP, the CYP inhibitory activities were different between the two compounds; compound **1** tended to inhibit CYP3A4 weaker than NVP (no significant difference) while compound **2** inhibited comparable to NVP. These results indicate that not only the quinone-methide intermediates but also other reactive metabolites might play an important role in NVP-induced CYP inhibition. Encouraged with this data, we also synthesized novel NVP analogs, which

modified the NVP A-ring to other heterocycles. Interestingly, the time-dependent CYP3A4 inhibition of the pyrimidine-analog **4** was significantly reduced, while those of the pyridine-analog **3** and the pyridazine-analog **5** were markedly increased in comparison with NVP. Although these compounds may form quinone-methide metabolites from a structural viewpoint, not all of these three compounds showed CYP inhibition. This also suggests the presence of an alternative reactive metabolite responsible for NVP-induced CYP inhibition outside of the quinone-methide intermediate. Considering that the *N*-methyl derivative **2** inhibited CYP3A4 at the same level as NVP, the quinone-methide intermediate is not thought to be the only contributor to NVP-induced CYP inhibition, since this type of reactive metabolite is difficult to be generated from compound **2**. On the other hand, reactive epoxide intermediates could be formed from all the tested compounds except for the pyrimidine-analog **4**. Based on this structural insight along with the results of the microsomal stabilities, the reactive epoxide intermediates of NVP might also be responsible for NVP-induced CYP inhibition. Indeed, Dekker et al. [20] reported that NVP-3-GSH derived from NVP-2,3-epoxide, not NVP-12-GSH derived from the quinone-methide intermediate, was the only GSH-conjugate detected when NVP was incubated with HLM and GSH.

Next, we examined the cytotoxicity of the synthesized compounds in a liver-derived cell line, HepG2 cells. HepG2 cells express little amount of CYP enzymes and are not appropriate to evaluate the toxicity of metabolites. Thus, we used TC-HepG2 cells expressing the four major CYP enzymes (CYP2C9, CYP2C19, CYP2D6, and CYP3A4). Unexpectedly, the cytotoxicity of NVP in TC-HepG2 cells was comparable to that in HepG2 cells (Fig. 4A, BSO (-)). This result raised the possibility that excess GSH levels in cells lessen the toxicity of NVP by trapping reactive NVP metabolites. Therefore, to definitively detect the toxicity being caused by reactive metabolites, we conducted cytotoxicity assays using BSO which inhibits GSH biosynthesis. By using a pretreatment of BSO, NVP-induced cytotoxicity was significantly increased in the TC-HepG2 cells when compared to the HepG2 cells and the BSO (-) group (Fig. 4A). These data indicates that the metabolism of NVP by CYP enzymes enhances NVP-induced cytotoxicity. Based on this result, we assessed the toxicity of the synthesized NVP analogs under depleted GSH conditions. For a comparison purpose, we also examined the toxicity without the pretreatment of BSO. As shown in Fig. 4B, compounds **3** and **4** significantly decreased toxicity when compared with NVP, and compounds **2** and **5** showed stronger toxicity than NVP in the BSO (+) condition, while such differences were not clearly observed in BSO (-) condition. This result also suggests that the remarkable toxicity of **2** and **5** may be due to their reactive metabolites detoxified by GSH in the same way as NVP and the BSO (+) condition is useful in order to compare the cytotoxicity of reactive metabolites formed from the synthesized compounds in the present study. The toxicity of desmethyl derivative **1** was comparable to NVP. Since the cytotoxicity of compounds **1** and **2** were similar to or stronger than that of NVP, it is suggested that a reactive epoxide intermediate, rather than a quinone-methide metabolite, may play an important role in NVP-induced cytotoxicity. Indeed, compounds **3** and **4**, which have difficulty generating reactive 2,3-epoxides, showed remarkably lower cytotoxicity than NVP. On the other hand, compound **5**, which was also thought to avoid the generation of the 2,3-epoxide, did not reduce the toxicity. As shown in Table 1, only compound **5** was metabolically unstable, and this might contribute to its cytotoxicity. The cytotoxicity of NVP analogs did not correlate completely with CYP inhibition such as compound **3** which showed more potent time-dependent CYP3A4 inhibition but lower cytotoxicity than NVP. These results might indicate that the key reactive metabolite is different between NVP-induced time-dependent CYP inhibition and hepatotoxicity.

Among the synthesized analogs, compound **4** which was designed to mitigate the formation of reactive epoxide metabolites tended to reduce the time-dependent CYP3A4 inhibition and TC-HepG2 cytotoxicity compared with NVP. Previously, Srivastava et al. showed that NVP-3-mercaptopurine, the *in vivo* metabolite produced via NVP-3-GSH, was detected as a major metabolite in urine of NVP-treated patients [10], while NVP-12-mercaptopurine was also detected from human urine. In addition, Dekker et al. [20] reported that NVP-3-GSH derived from NVP-2,3-epoxide was the only GSH-conjugate detected in HLM fortified with GSH as described above. Considering these reports and the present study together, it is possible that the reactive epoxide metabolite of NVP may play a significant role in the liver toxicity in human.

In the current study, we examined time-dependent CYP inhibition and cytotoxicity in liver-derived cells to evaluate the metabolic activation of compounds. However, it is widely accepted that the emergence of drug-induced liver injury is thought to be a more complex process and associated with an immune-mediated pathway. Further studies are needed to fully understand the significance of the reactive epoxide metabolite in the liver toxicity induced by NVP.

In conclusion, we have synthesized five NVP analogs in order to identify the reactive metabolite of NVP mainly responsible for NVP-induced liver injury. The present study indicates that an alternative pathway, in which a reactive epoxide intermediate is generated, might play an important role in the metabolic activation of NVP.

#### Authorship contributions

Participated in research design: Tateishi, Ohe, Takahashi, Yasuda, Nakamura and Mashino.

Conducted experiments: Tateishi.

Contributed reagents or analytical tools: Kazuki.

Performed data analysis: Tateishi.

Wrote or contributed to the writing of the manuscript: Tateishi, Ohe and Mashino.

All authors provided final approval of the manuscript.

#### Declaration of competing interest

The authors declare no conflict of interest.

#### Acknowledgement

This research was supported by Platform Project for Supporting Drug Discovery and Life Science Research (Basis for Supporting Innovative Drug Discovery and Life Science Research (BINDS)) from AMED under Grant Number JP19am0101089 (M.T.) and JP19am0101124 (Y.K.). This work was also supported by JSPS KAKENHI (Grant Number 16K08379) and a special grant generously provided by the Hoansha Foundation.

#### Appendix A. Supplementary data

Supplementary data to this article can be found online at <https://doi.org/10.1016/j.dmpk.2020.01.006>.

#### References

- Pollard RB, Robinson P, Dransfield K. Safety profile of nevirapine, a non-nucleoside reverse transcriptase inhibitor for the treatment of human immunodeficiency virus infection. *Clin Therapeut* 1998;20:1071–92. [https://doi.org/10.1016/S0149-2918\(98\)80105-7](https://doi.org/10.1016/S0149-2918(98)80105-7).
- Fang JL, Beland FA. Differential responses of human hepatocytes to the non-nucleoside HIV-1 reverse transcriptase inhibitor nevirapine. *J Toxicol Sci* 2013;38:741–52. <https://doi.org/10.2131/jts.38.741>.
- Wongtrakul J, Paemanee A, Wintachai P, Thepparit C, Roytrakul S, Thongtan T, et al. Nevirapine induces apoptosis in liver (HepG2) cells. *Asian Pac J Trop Med* 2016;9:547–53. <https://doi.org/10.1016/j.apjtm.2016.04.015>.
- Paemanee A, Sornjai W, Kittisenachai S, Sirinonthanawech N, Roytrakul S, Wongtrakul J, et al. Nevirapine induced mitochondrial dysfunction in HepG2 cells. *Sci Rep* 2017;7:9194. <https://doi.org/10.1038/s41598-017-09321-y>.
- Riska P, Lamson M, Macgregor T, Sabo J, Hattos S, Pav J, et al. Disposition and biotransformation of the antiretroviral drug NVP in humans. *Drug Metab Dispos* 1999;27:895–901.
- Erickson DA, Mather G, Trager WF, Levy RH, Keirns JJ. Characterization of the *in vitro* biotransformation of the HIV-1 reverse transcriptase inhibitor nevirapine by human hepatic cytochromes P-450. *Drug Metab Dispos* 1999;27:1488–95.
- Chen J, Mannargudi BM, Xu L, Uetrecht JP. Demonstration of the metabolic pathway responsible for nevirapine-induced skin rash. *Chem Res Toxicol* 2008;21:1862–70. <https://doi.org/10.1021/tx800177k>.
- Caixas U, Antunes AMM, Marinho AT, Godinho ALA, Grilo NM, Marques MM, et al. Evidence for nevirapine bioactivation in man: searching for the first step in the mechanism of nevirapine toxicity. *Toxicology* 2012;301:33–9. <https://doi.org/10.1016/j.tox.2012.06.013>.
- Meng X, Howarth A, Earnshaw CJ, Jenkins RE, French NS, Back DJ, et al. Detection of drug bioactivation *in vivo*: mechanism of nevirapine-albumin conjugate formation in patients. *Chem Res Toxicol* 2013;26:575–83. <https://doi.org/10.1021/tx4000107>.
- Srivastava A, Lian LY, Maggs JL, Chaponda M, Pirmohamed M, Williams DP, et al. Quantifying the metabolic activation of nevirapine in patients by integrated applications of NMR and mass spectrometry. *Drug Metab Dispos* 2010;38:122–32. <https://doi.org/10.1124/dmd.109.028688>.
- Sharma AM, Klarskov K, Uetrecht JP. Nevirapine bioactivation and covalent binding in the skin. *Chem Res Toxicol* 2013;26:410–21. <https://doi.org/10.1021/tx3004938>.
- Sharma AM, Novalen M, Tanino T, Uetrecht JP. 12-OH-nevirapine sulfate, formed in the skin, is responsible for nevirapine-induced skin rash. *Chem Res Toxicol* 2013;26:817–27. <https://doi.org/10.1021/tx400098z>.
- Zhang X, Sharma AM, Uetrecht JP. Identification of danger signals in nevirapine-induced skin rash. *Chem Res Toxicol* 2013;26:1378–83. <https://doi.org/10.1021/tx400232s>.
- Fang JL, Loukotková L, Chitranshi P, Gamboa da Costa G, Beland FA. Effects of human sulfotransferases on the cytotoxicity of 12-hydroxynevirapine. *Biochem Pharmacol* 2018;155:455–67. <https://doi.org/10.1016/j.bcp.2018.07.016>.
- Sharma AM, Li Y, Novalen M, Hayes MA, Uetrecht JP. Bioactivation of nevirapine to a reactive quinone methide: implications for liver injury. *Chem Res Toxicol* 2012;25:1708–19. <https://doi.org/10.1021/tx300172s>.
- Harjivan SG, Pinheiro PF, Martins IL, Godinho AL, Wanke R, Santos PP, et al. Quinoid derivatives of the nevirapine metabolites 2-hydroxy- and 3-hydroxy-nevirapine: activation pathway to amino acid adducts. *Toxicol Res (Camb)* 2015;4:1565–77. <https://doi.org/10.1039/c5tx00176e>.
- Satoh D, Iwado S, Abe S, Kazuki K, Wakuri S, Oshimura M, et al. Establishment of a novel hepatocyte model that expresses four cytochrome P450 genes stably via mammalian-derived artificial chromosome for pharmacokinetics and toxicity studies. *PLoS One* 2017;12. <https://doi.org/10.1371/journal.pone.0187072>.
- Wen B, Chen Y, Fitch WL. Metabolic activation of nevirapine in human liver microsomes: dehydrogenation and inactivation of cytochrome P450 3A4. *Drug Metab Dispos* 2009;37:1557–62. <https://doi.org/10.1124/dmd.108.024851>.
- Hargrave KD, Proudfoot JR, Grozinger KG, Cullen E, Kapadia SR, Patel UR, et al. Novel non-nucleoside inhibitors of HIV-1 reverse transcriptase. 1. Tricyclic pyridobenzo- and dipyrindiazepinones. *J Med Chem* 1991;34:2231–41. <https://doi.org/10.1021/jm00111a045>.
- Dekker SJ, Zhang Y, Vos JC, Vermeulen NPE, Commandeur JNM. Different reactive metabolites of nevirapine require distinct glutathione S-transferase isoforms for bioactivation. *Chem Res Toxicol* 2016;29:2136–44. <https://doi.org/10.1021/acs.chemrestox.6b00250>.